Relativistic many-body approach to hyperfine interaction in rare earths: Explanation of experimental result in europium*

J. Andriessen
Laboratorium voor Technische Natuurkunde, Technische Hogeschool, Delft, Netherlands

K. Raghunathan, S. N. Ray, and T. P. Das
Department of Physics, State University of New York, Albany, New York 12222

(Received 19 May 1976)

A first-principles relativistic many-body treatment is carried out for the hyperfine constant in europium atom. This investigation has allowed us to sort out for the first time all the contributing physical mechanisms, core polarization, correlation, relativistic modifications of these, and the purely relativistic Casimir and breakdown of *LS* coupling effects. It is found that all these competing contributions have to be accurately evaluated to successfully explain the observed small hyperfine constant.

I. INTRODUCTION

The hyperfine constant of europium atom was measured[1] almost a decade back but a quantitative understanding of it has remained elusive so far. The reasons for this can be appreciated by an examination of the relative sizes of some of the contributions that have been considered previously, as compared to the experimental result. The experimental value[1] of the hyperfine constant for ^{153}Eu is -8.8532 ± 0.0002 MHz, which should be compared with an earlier calculation[2] of the exchange-core polarization[3] (ECP) contribution of -35 MHz, composed of substantial contributions of opposing sign from individual shells, for example, -182, -181, and 275 MHz from the $3s$, $4s$, and $5s$ shells, respectively.

Two other mechanisms proposed by Sandars and Beck[4] are the breakdown of *LS* coupling (BDLSC) and the Casimir effects, both of which result from the nonsphericity of the $4f^7$ shell in relativistic theory. A more-recent[5] relativistic Hartree-Fock calculation of these latter effects led to contribution of 3.9 and -17.8 MHz, respectively, their sum of -13.9 MHz being of comparable order as the experimental hyperfine constant. A situation of this kind, involving a relatively small experimental hyperfine constant and a number of competing mechanisms with comparable or substantially larger contributions, requires that all such contributions be obtained accurately in order to have a complete explanation of the experimental result. Thus in the case of phosphorus atom, it was crucial to incorporate[6] correlation effects to bridge the gap between the experimental value[7] and the value arising from one-electron theory. Also a recent investigation[8] on manganese atom has shown that the relativistic enhancements of one- and many-electron contributions were important to obtain agreement with the experimental hyperfine constant.[9]

The rare-earth atoms being heavier usually involve more significant cancellations[3] among individual shells and are expected to have more pronounced relativistic effects. In the present work we have therefore carried out a complete relativistic many-body analysis of the hyperfine interaction in europium using the linked-cluster many-body perturbation-theory (LCMBPT) procedure.[10]

Further in order to obtain valuable insight into the role of relativistic effects on various mechanisms, we have also carried out a complete nonrelativistic LCMBPT analysis, which has enabled a comparison of corresponding relativistic and nonrelativistic diagrams. The information obtained from the present analysis regarding the importance of relativistic effects as well as other mechanisms such as ECP and correlation effects is expected to be of general value for the understanding of these effects in other rare-earth systems both in the free state as well as in solids.

The various physical mechanisms that contribute to the hyperfine constant are considered in Sec. II. Also the procedures for evaluating these diagrams in both the relativistic and nonrelativistic cases are briefly discussed. Section III presents the results for the contributions from the various mechanisms in both relativistic and nonrelativistic theory. These results permit us to draw conclusions regarding the relative importance of all the physical mechanisms and the influence of relativistic effects on them. Following this a comparison is made between the experimental hyperfine constant and our net theoretical result after careful consideration of the accuracy of the latter.

II. THEORY

We briefly describe first the formalism and procedure for the calculation in order to facilitate the presentation of the mechanisms and their contributions to the hyperfine constant. The Hamiltonian for the many-electron atom can be written as follows:

$$H = H_0 + H' . \tag{1}$$

The zero-order Hamiltonian H_0 in the single particle approximation is chosen to have the V^{n-1} form

$$H_0 = \sum_{i=1}^{N} h_0(i) = \sum_{i=1}^{N} \left[-\tfrac{1}{2}\nabla_i^2 + v(i) \right], \tag{2}$$

where the summation over i runs over all the N electrons in the atom and the matrix elements of the one-electron potential v are given by

$$\langle a | v | b \rangle = \sum_{n=1}^{N-1} \langle an | v | bn \rangle - \langle an | v | nb \rangle . \tag{3}$$

In Eq. (3) the one-electron states n refer to the Hartree-Fock states of the atom. In the relativistic case, the corresponding H_0 is given by

$$H_0 = \sum_{i=1}^{N} h_0(i) = \sum_{i=1}^{N} \left[c\vec{\alpha}_i \cdot \vec{p}_i + \beta_i m + w(i) \right]. \tag{4}$$

The matrix elements of w are given by an equation identical to (3) but with the states n replaced by the four-component relativistic states obtained by the prescription of Andriessen and Van Ormondt[11] and utilized in the recent work on manganese atom.[8] The perturbation Hamiltonian H' is given by

$$H' = \sum_{i>j} \frac{1}{r_{ij}} - \sum_i V_i^{N-1}, \tag{5}$$

V_i^{N-1} being the chosen one-electron potentials corresponding to H_0 in Eqs. (2) and (4).

The basis sets needed for the LCMBPT procedure are generated by solving the one-electron equations corresponding to H_0. For the relativistic case the one-electron basis states are the four component jm states. The unperturbed ground states Φ_0 of the many-electron system is constructed for both the nonrelativistic and the relativistic cases through appropriate occupation of the one-electron basis states.

For studying hyperfine properties, one needs the expectation value of the hyperfine Hamiltonian H_N over the exact ground-state wave function of the Hamiltonian H of Eq. (1) for the atom. Because of the spherical nature of the ground state of Eu^0 in the nonrelativistic approximation, the electron-nuclear dipole hyperfine interaction does not make any contribution and only the contact term[10]

$$H_N = \frac{8\pi}{3} \frac{\mu_B \mu_N}{I a_b^3} \vec{I} \cdot \sum_{i=1}^{N} 2\vec{s}_i \delta(r_i) \tag{6}$$

has to be considered. For the relativistic case H_N is given by[12]

$$H_N = -e \sum_{i=1}^{N} \vec{\alpha}_i \cdot \left(\frac{\vec{\mu}_I \times \vec{r}_i}{r_i^3} \right), \tag{7}$$

where α_i are the Dirac matrices and μ_I is the nuclear magnetic moment. The relativistic H_N includes the dipolar and the orbital terms along with the contact term.

Using the linked-cluster expansion, the expectation value of the hyperfine Hamiltonian H_N over the ground state of H can be written[10]

$$\langle H_N \rangle = \sum_{m,n=0}^{\infty} \langle \Phi_0 | \left(\frac{H'}{E_0 - H_0} \right)^n H_N \left(\frac{H'}{E_0 - H_0} \right)^m | \Phi_0 \rangle_L . \tag{8}$$

The subscript L denotes that only the linked diagrams have to be considered in each order. The diagrams representing the various terms in a given order of the perturbation expansion are labeled by the pair of indices (n, m).

In the nonrelativistic case the contributions from the lowest order (0, 0) vanish both because of the sphericity of the ground state and because the $4f$ electrons have no density at the nucleus and so cannot contribute to the contact interaction. In the relativistic case, however, one does get a finite contribution in lowest order because of the lack of sphericity of the ground state due to two types of spectroscopic term mixing. It can be shown[11] that there is term-mixing both from within the $4f^7$ configuration and outside this configuration. These two types of mixing lead to the two mechanisms referred to in the literature[4] as BDLSC and Casimir effects, respectively. These effects are represented in Fig. 1(a), the one-electron state in this diagram referring to the relativistic $4f$ state constructed according to the prescription of Andriessen and Van Ormondt.

In the next order of perturbation (0, 1) we get the ECP contribution given by the diagram of Fig. 1(b). In this order and in all higher ones the hole states in the diagrams that correspond to the $4f$ shell are chosen according to the prescription of Andriessen and Van Ormondt while the rest of the hole and particle states are jm states. It should be noted that in the relativistic approach the hole states in Fig. 1(b) can be $p_{1/2}$ states in addition to being $s_{1/2}$ states, the latter ones being the only ones that contribute in nonrelativistic theory.

In the second order of perturbation there are two types of terms, (0, 2) and (1, 1). Each of these types is composed of two classes, namely, the one-electron consistency and the dynamic-correlation diagrams. The former class corrects the potential felt by one electron in some orbital for the

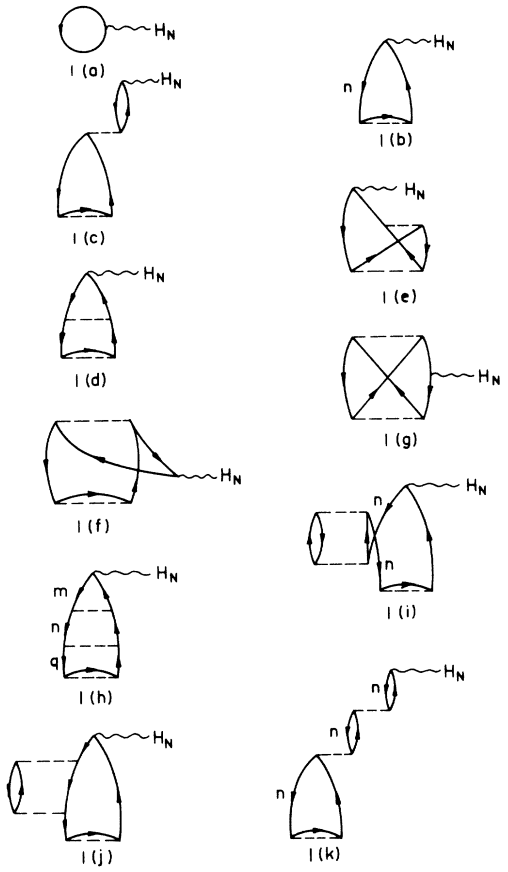

FIG. 1. Typical hyperfine diagrams of various orders for Eu^0 atom.

changes in the orbitals of the other electrons produced by the magnetic hyperfine interaction. The dynamic correlation diagrams represent mixing into the ground state of states in which two electrons are simultaneously excited. Typical consistency and correlation diagrams of these orders are shown, respectively, in Figs. 1(c), 1(d), and 1(e) and Figs. 1(f) and 1(g). The important diagrams beyond second order are represented by Figs. 1(h)–1(k). Of these higher-order diagrams, in the type 1(h), the class with $m=n=q$ are combined with the diagram 1(d) with $m=n$ to give ladder corrections[8,10] to the (0, 1) ECP diagram. These ladder corrections are characteristic of the chosen V^{N-1} potential. The class of diagram 1(h) with $m=n\neq q$ was also included as a similar ladder correction to the (0, 2) consistency contributions. The rearrangement diagram 1(i) on the other hand, represents the influence of pair correlations among the electrons on the ECP diagram 1(b). The influence of these pair correlations is included to all orders as a shift in the energy of state n occurring in the energy denominator for diagram 1(b). The remaining higher-order diagrams in Fig. 1 are those of the type 1(h) with $m\neq n$, and 1(j) and 1(k). The evaluation of these higher-order diagrams and comparison with the corresponding lower-order ones such as, for instance, 1(k) with 1(c), allows one to estimate the possible importance of the rest of the higher-order diagrams that are not included in our work. This is necessary for estimating the confidence limit of our theoretical result for the hyperfine constant.

TABLE I. Contributions to the hyperfine constant of ^{153}Eu atom (in MHz) from relativistic and nonrelativistic diagrams.

Perturbation order	Mechanism	Relativistic result I	Nonrelativistic result II	Relativistic enhancement I-II
Zero order	Casimir	−12.9	···	−12.9
(0, 0)	BDLSC	3.0	···	3.0
First order	ECP s type $1s$	0.1	0.1	
(0, 1)	$2s$	5.7	1.5	
	$3s$	−215.3	−189.4	
	$4s$	−337.9	−189.1	
	$5s$	398.0	253.6	
	$6s$	79.1	40.2	
	Total	−70.3	−83.1	12.8
	p type	3.0	···	3.0
Second order	Consistency	55.5	36.8	18.7
(1, 1) + (0, 2)	Correlation	6.9	−1.4	8.3
Higher order		3.9	2.7	1.2
Total		−10.9	−45.0	34.1
Experiment		−8.8532 ± 0.0002		

III. RESULTS AND DISCUSSION

Before entering into comparison between the net theoretical result and the experimental result we like to discuss some features of the contributions from various mechanisms, listed in Table I. Our results for zero order from Casimir and BDLSC effects differ from those of the earlier relativistic-Hartree-Fock calculation,[5] since there only one of the possible configurations in jj coupling was used in constructing the potential for generating the one-electron states belonging to the $4f$ shell.

Turning next to first order, the individual shell and net s-type ECP contributions are listed in Table I. The latter includes both the sum of the individual shell contributions as well as ladder and rearrangement corrections. It is remarkable that the net relativistic result is substantially smaller than the nonrelativistic counterpart, unlike what one expects from the increase[13] in the s-state densities at the nucleus due to the contraction from relativistic effects. This feature of the ECP result is a consequence of the combination of two facts.[8,14] The first is that the ECP contributions from individual shells vary in sign as seen from Table I. The second is that while due to relativistic effects, the densities of the individual shells at the nucleus always increase, the exchange interaction of the various s shells with the $4f$ electrons can either increase or decrease. The p-type ECP contribution as remarked in Sec. II occurs only in relativistic theory.

The consistency and correlation contributions in Table I are obtained by evaluating all the corresponding second-order diagrams (typical ones being represented in Figs. 1(c)–1(g) and the corresponding ladders. The net consistency effect is much stronger than the net correlation effect in both relativistic and nonrelativistic cases. Though the individual correlation diagrams are substantial, the net result is small due to cancellations among them. This cancellation also leads to the interesting reversal in sign between the relativistic and the nonrelativistic correlation contributions.

The results in Table I, listed under higher-order contributions, refer to those higher-order diagrams in Fig. 1 that were not included as ladder or rearrangement corrections, that is, to a combination of the correlation-type diagram 1(k), and the consistency type diagram 1(j), and those of the type 1(h) in which $m \neq n$. This higher-order contribution is seen to be substantially smaller than the sum of the consistency and correlation contributions grouped under second order in Table I. Considering the fact that the higher-order diagrams individually were also found to be rather small and that the higher-order contribution is only 1% of the largest of the ECP contributions (from $5s$) indicates that the perturbation series has indeed converged satisfactorily.

In view of the strong cancellations seen in Table I between the ECP contributions from various core ns shells and between the different mechanisms, it is important to estimate a confidence limit for our net theoretical result. For this we first consider the influence of higher-order diagrams not included in this work. An examination of the relative importance of higher-order diagrams included in Table I, as compared to their lowest-order counterparts, and of the magnitudes of other typical higher-order ones not included in Table I, leads us to ascribe a confidence limit of ±1 MHz from this source. The other important source to be considered in obtaining the confidence limit is the influence of limitations in the computational techniques. We have made a conservative estimate of ±2 MHz for this contribution, through evaluation of some of the larger (0, 1) diagrams by an alternative method.[15] From these considerations we estimate the confidence limit of our result to be ±3 MHz. The experimental result is seen from Table I to agree well with our theoretical result within the confidence limit.

In conclusion, the present study has provided good agreement with experiment for the hyperfine constant in europium atom, which has perhaps the severest known cancellations among the various contributions to the hyperfine constant. Further, the analysis of all the one-electron and many-electron contributions studied here in both relativistic and nonrelativistic theories, suggests that in general for all rare-earth systems the quantitative understanding of the hyperfine constants would require the incorporation of all these contributions using relativistic theory. The relativistic LCMBPT procedure developed and applied here appears to be well suited for such a task for all rare-earth atoms and ions in free state. For rare-earth compounds one has to complement this procedure by inclusion of covalency effects.

*Supported by NSF and The Netherlands Organization of Pure Scientific Research.

[1]F. M. Pichanick, P. G. H. Sandars, and G. K. Woodgate, Proc. R. Soc. Lond. A 257, 277 (1960); L. Evans, P. G. H. Sandars, and G. K. Woodgate, *ibid.* 289, 144 (1965).

[2]D. Ikenberry, T. P. Das, and J. B. Mann, Phys. Rev. A 4, 2188 (1971).

[3]R. E. Watson and A. J. Freeman, in *Hyperfine Interactions*, edited by A. J. Freeman and R. B. Frankel (Academic, New York, 1967).

[4]P. G. H. Sandars and J. Beck, Proc. R. Soc. Lond. A 289, 97 (1905).

[5]M. A. Coulthard, Proc. Phys. Soc. Lond. 90, 615 (1967). The values quoted in this paper correspond to ^{153}Eu.

[6]N. C. Dutta, C. Matsubara, R. T. Pu, and T. P. Das, Phys. Rev. Lett. 21, 1139 (1968).

[7]J. M. Pendlebury and K. F. Smith, Proc. Phys. Soc. Lond. 84, 849 (1969); R. H. Lambert and F. M. Pipkin, Phys. Rev. 128, 198 (1962).

[8]J. Andriessen, S. N. Ray, T. Lee, T. P. Das, and D. Ikenberry, Phys. Rev. A 13, 1669 (1976).

[9]S. J. Davis, J. J. Wright, and L. C. Balling, Phys. Rev. A 3, 1220 (1971); G. K. Woodgate and J. S. Martin, Proc. Phys. Soc. Lond. A 70, 485 (1957).

[10]See, for example, S. N. Ray, T. Lee, and T. P. Das, Phys. Rev. B 8, 5291 (1973), and references therein.

[11]J. Andriessen and D. Van Ormondt, J. Phys. B 8, 1993 (1975).

[12]See, T. P. Das, *Relativistic Quantum Mechanics of Electrons* (Harper and Row, New York, 1973), Chap. 7.

[13]A. Trautwein, Frank E. Harris, A. J. Freeman, and J. P. Desclaux, Phys. Rev. B 11, 4101 (1975).

[14]J. Andriessen, D. Van Ormondt, S. N. Ray, K. Raghunathan, and T. P. Das, Bull. Am. Phys. Soc. 21, 12 (1976).

[15]The 4*s* and 5*s* ECP contributions were compared with the corresponding results obtained by direct numerical integration of the appropriate exchange perturbation equations [see, for example, K. J. Duff and T. P. Das, Phys. Rev. 168, 43 (1968) for the nonrelativistic counterpart].